Cosmological Applications of a Wavelet Analysis on the Sphere

J. D. McEwen, P. Vielva, Y. Wiaux, R. B. Barreiro, L. Cayón, M. P. Hobson, A. N. Lasenby, E. Martínez-González, and J. L. Sanz

Communicated by Jean-Pierre Antoine

ABSTRACT.   *The cosmic microwave background (CMB) is a relic radiation of the Big Bang and as such it contains a wealth of cosmological information. Statistical analyses of the CMB, in conjunction with other cosmological observables, represent some of the most powerful techniques available to cosmologists for placing strong constraints on the cosmological parameters that describe the origin, content and evolution of the Universe. The last decade has witnessed the introduction of wavelet analyses in cosmology and, in particular, their application to the CMB. We review here spherical wavelet analyses of the CMB that test the standard cosmological concordance model. The assumption that the temperature anisotropies of the CMB are a realisation of a statistically isotropic Gaussian random field on the sphere is questioned. Deviations from both statistical isotropy and Gaussianity are detected in the reviewed works, suggesting more exotic cosmological models may be required to explain our Universe. We also review spherical wavelet analyses that independently provide evidence for dark energy, an exotic component of our Universe of which we know very little currently. The effectiveness of accounting correctly for the geometry of the sphere in the wavelet analysis of full-sky CMB data is demonstrated by the highly significant detections of physical processes and effects that are made in these reviewed works.*

1.   Introduction

A concordance model of modern cosmology has emerged only recently, explaining many different observations of our Universe to very good approximation. The Λ Cold Dark Matter

---

(ΛCDM) cosmological concordance model is characterised by a universe consisting of ordinary baryonic matter, cold dark matter and dark energy (represented by the cosmological constant Λ). Current estimates place the relative contributions of these components at 4%, 22%, and 74% of the energy density of the Universe, respectively, [43]. Cold dark matter consists of nonrelativistic, nonbaryonic patricles that interact gravitationally only. Although dark matter has yet to be observed directly, its presence has been inferred from a range of observations, such as galaxy rotation curves and the formation of the large scale structure of our Universe. Dark energy characterises the intrinsic nature of space to expand and may represent the energy density of empty space. Although the origin and nature of dark energy remains unclear, it may be modelled by a cosmological fluid with negative pressure, acting as a repulsive force counteracting the attractive nature of the gravitational interaction of matter. Dark energy is required to explain the accelerating expansion of our Universe apparent from supernovae observations. Strong evidence supporting the ΛCDM model is also provided by observations of the cosmic microwave background (CMB), the relic radiation of the Big Bang. The model not only predicts the existence of the CMB but it also describes, to very high accuracy, the acoustic oscillations imprinted in the temperature fluctuations of the CMB.

An era of precision cosmology is emerging in which many cosmological parameters of the ΛCDM model are constrained to high precision. Although the cosmological concordance model is well grounded both theoretically and empirically, the finer details of the model are still under much debate. The observable predictions made by different cosmological scenarios vary only slightly, however the models themselves can have wide ranging implications for the nature of our Universe. Due to recent high-precision data-sets and well grounded analysis techniques, precision cosmology is beginning to allow the finer cosmological details to be tested. Independent confirmation of the general model is of particular importance also. In this review we concentrate on analyses of the CMB that apply wavelets on the sphere to test and constrain the cosmological concordance model.

CMB photons were emitted when the Universe was just one fifty-thousandth of its present age and since have travelled largely unhindered through our Universe, redshifting along with the expansion of the Universe. These photons are observed today in the microwave range, exhibiting a near-perfect black-body spectrum with a mean temperature of 2.73K. Observations of the CMB provide a unique imprint of the early Universe. The CMB is highly isotropic, with temperature anisotropies originating from primordial perturbations at a level of 10^{-5} only. However, these small temperature anisotropies contain a wealth of cosmological information. The temperature anisotropies of the CMB are thought to be a realisation of a statistically isotropic (i.e., stationary) Gaussian random field over the sphere. Observations of the CMB are made on the celestial sphere since, due to the original singularity and subsequent expansion of the Universe, CMB photons travel towards us from all directions. A full-sky map of the CMB temperature anisotropies measured by NASA's Wilkinson Microwave Anisotropy Probe (WMAP) satellite [22] is illustrated in Figure 1. When analysing a full-sky CMB map, the geometry of the sphere must be taken into account.

Wavelets are a powerful signal analysis tool owing to the simultaneous spatial and scale localisation encoded in the analysis. In order to realise the potential benefits of a wavelet analysis of full-sky CMB maps it is necessary to employ a wavelet analysis defined on a spherical manifold. Early attempts at applying wavelets to spherical CMB maps were performed by [4, 12, 11]. In this review. however, we focus on cosmological applications that employ the wavelet transform on the sphere constructed by [3, 2]. This methodology was derived originally entirely from group theoretical principles. However, in a recent
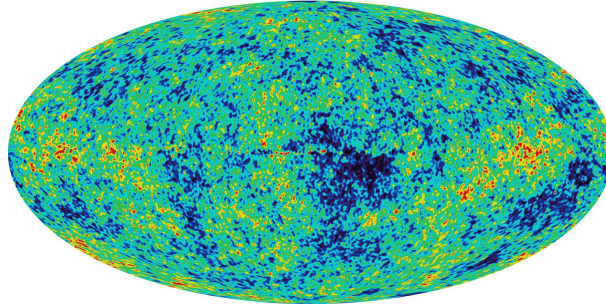
FIGURE 1   Full-sky map of the CMBanisotropies measured by WMAP (courtesy of the WMAPscience team: `http://map.gsfc.nasa.gov/`). The Mollweide projection is used here and subsequently to display data defined on the sphere.

work by [48] this formalism is reintroduced independently of the original group theoretic formalism, in an equivalent, practical and self-consistent approach. Application of this wavelet framework on the sphere for large data-sets has been prohibited previously by the computational infeasibility of any implementation. Two fast algorithms have been derived recently to perform a general directional wavelet analysis on the sphere [32, 49]. Without such algorithms, cosmological analyses would not be computationally feasible due to the large size of current and forthcoming CMB data-sets, such as the 3 mega-pixel WMAP maps and 50 mega-pixel Planck [38] maps, respectively. These fast algorithms and the wavelet methodology derived by [48] are reviewed in another article of the present issue [50].

A number of analyses of the CMB have been performed using wavelets on the sphere to test and constrain the cosmological concordance model that describes our Universe. The importance of accounting correctly for the geometry of the sphere is demonstrated in these analyses by the highly statistically significant detections of physical processes that have been made. In this review we discuss a selection of these analyses. In Section 2 we review works that test the hypothesis that the CMB temperature anisotropies are indeed a realisation of a Gaussian random field on the sphere. These works highlight slight deviations from Gaussianity and flag localised non-Gaussian features in the CMB, thereby providing evidence for nonstandard cosmological models. In Section 3 we review work to test the statistical isotropy (i.e., stationarity) of the CMB temperature anisotropies, another assumption of the standard cosmological concordance model. Unexplained deviations from isotropy are detected, suggesting the need for possible alterations to the standard cosmological model. In the final cosmological application of a wavelet analysis on the sphere that we review, we focus on verifying the existence of dark energy in the concordance model. In Section 4 we review works that use an independent method to provide evidence for dark energy and constrain its relative abundance in the Universe. Concluding remarks are made in Section 5.

2.   Gaussianity of the CMB

A range of primordial processes may imprint signatures on the temperature fluctuations of the CMB. The currently favoured cosmological concordance model is based on the assumption of initial fluctuations generated by inflation. In the simplest inflationary models, primordial perturbations seed Gaussian temperature fluctuations in the CMB that are statistically isotropic over the sky. However, this is not necessarily the case in, for ex-

ample, nonstandard inflationary models or various cosmic defect scenarios. Moreover, non-Gaussianity may also be introduced in observational data by secondary physical effects, residual foregrounds and instrumental systematics. Testing whether the temperature anisotropies of the CMB are a realisation of a Gaussian random field is of considerable interest. Departures from this assumption would either provide evidence for competing scenarios of the early Universe, highlight important secondary sources of non-Gaussianity or highlight the presence of spurious signals due to foregrounds or systematic effects.

The assumption of Gaussianity has been questioned recently with many works detecting deviations from Gaussianity in the WMAP data (for a review see [28]). Although the departures from Gaussianity detected in the WMAP data may simply highlight unremoved foreground contamination or other systematics in the data, which themselves are of importance for cosmological inferences drawn from the data, if the source of these detections is of cosmological origin then this would have important implications for the standard cosmological model.

Ideally, one would like to localise any detected non-Gaussian regions of the CMB on the sky, in particular to determine whether they correspond to secondary effects or systematics. The ability to probe different scales is also important to ensure that non-Gaussian sources present only on certain scales are not concealed by the predominant Gaussianity of other scales. Wavelet techniques are thus a perfect candidate for CMB non-Gaussianity analysis. Many detections of deviations from Gaussianity have been made in the WMAP data, some of the most significant of which have been obtained using spherical wavelets [10, 44, 34, 29, 17, 18, 16, 30]. Moreover, the wavelet analysis has allowed those regions that are most likely to induce non-Gaussianity to be localised on the sky. In the remainder of this section we review these analyses, focusing on the work performed in [44, 29, 30]. We review the analysis procedure performed, the deviations from Gaussianity observed and the localised non-Gaussian regions detected.

2.1 Analysis Procedure

The wavelet transform is a linear operation. Consequently, the wavelet coefficients of a Gaussian map will also follow a Gaussian distribution. One may therefore probe a full-sky CMB map for non-Gaussianity simply by looking for deviations from Gaussianity in the distribution of its spherical wavelet coefficients. Sky-cuts that would otherwise introduce non-Gaussianity may be easily accounted for by excluding those coefficients corresponding to wavelets that significantly overlap the mask. The analysis procedure consists of first taking the spherical wavelet transform of the WMAP data at a range of scales. Wavelet dilation scales of $14'$–$1000'$ are considered in [44], whereas in [29, 30] the analysis is focused on the scales where non-Gaussianity was detected by [44], i.e., on wavelet scales ranging from $50'$–$600'$. The effective size of a wavelet on the sky is approximately twice the wavelet dilation. Five evenly spaced azimuthal γ orientations in the domain $[0, \pi)$ are considered for the directional wavelets applied in [29, 30].[1] Skewness and excess kurtosis test statistics are calculated from the wavelet coefficients in order to examine the Gaussianity of the data. For a Gaussian distribution skewness and excess kurtosis are zero, hence any deviation from zero in these wavelet statistics, on any particular scale

---

[1]Identical orientations are considered at each point in the analysis performed by [29, 30], in contrast to a continuous orientational analysis that could be performed using steerable wavelets [50]. The latter approach is the focus of current work.

or orientation, highlights possible deviations from Gaussianity in the CMB temperature anisotropies. Monte Carlo simulations are performed to construct significance measures for any candidate deviations from Gaussianity. Gaussian simulations of CMB data are constructed that model carefully the WMAP observing strategy. An identical analysis to that performed on the WMAP data is applied to the simulated CMB maps, in order to constrain the significance of any detections of non-Gaussianity made from the data. Positive detections of deviations from Gaussianity are then used to localise regions on the sky that are the most likely sources of any non-Gaussian signal observed.

2.2 Results and Discussion

We review here the detections of non-Gaussianity made using the spherical Mexican hat wavelet (SMHW) and the directional spherical Morlet wavelet (SMW) (see [50] for definitions and illustrations of these wavelets). The test statistics corresponding to the most significant detections of deviations from Gaussianity are displayed in Figure 2, with confidence intervals constructed from Monte Carlo simulations also shown. Deviations from Gaussianity are observed well outside of the 99% confidence region for both wavelets. The most significant detection made with the SMHW occurs in the kurtosis of wavelet coefficients, whereas the most significant detection made with the SMW occurs in the skewness. On examining the statistical significance of detections in more detail, the deviations from Gaussianity are made at 99.9% and 99.3% using the SMHW and the SMW, respectively, using a χ^2 test based on the aggregate set of skewness and kurtosis test statistics to compute these significance levels.

(a) SMHW kurtosis
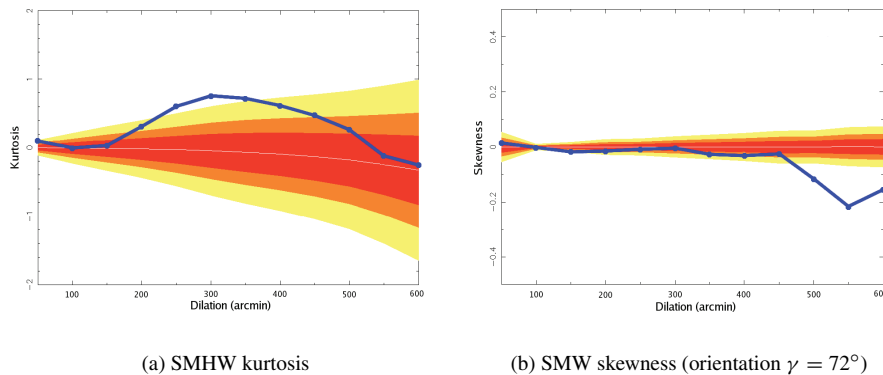
(b) SMW skewness (orientation $\gamma = 72°$)

FIGURE 2   Spherical wavelet coefficient statistics for each wavelet. Confidence regions obtained from 1000 Monte Carlo simulations are shown for 68% (dark grey), 95% (grey) and 99% (light grey) levels, as is the mean (solid white line). Only the orientation corresponding to the most significant deviation from Gaussianity is shown for the directional SMW.

A wavelet analysis inherently allows the spatial localisation of interesting signal characteristics. The most pronounced deviations from Gaussianity in the WMAP data may therefore be localised on the sky. For each wavelet, the wavelet coefficients corresponding to the most significant detection of non-Gaussianity are displayed in Figure 3, accompanied by corresponding thresholded coefficient maps to localise the most pronounced deviations

from Gaussianity. To investigate the impact of these localised regions on the initial detections of non-Gaussianity, the corresponding coefficients are removed from the calculation of skewness and kurtosis test statistics. After making this correction the non-Gaussian signals detected by each wavelet (Figure 2) are eliminated completely. The localised regions identified do indeed appear to be the source of the non-Gaussianity detected. In a continuation of the work of [44], the localised regions detected by the SMHW analysis are examined in more detail in [17, 18, 16, 10]. The large cold spot at Galactic coordinates $(l, b) = (209°, -57°)$ is found to be the predominant source of non-Gaussianity detected in the kurtosis of the SMHW coefficients. When this cold spot is removed the kurtosis of SMHW coefficients is consistent with Gaussianity. The cold spot appears to be an anomalous region on the sky not consistent with Gaussian CMB temperature anisotropies, however its origin remains unknown. Possible origins of the cold spot remain the focus of current research.

(a) SMHW coefficients (dilation 300′)

(b) SMW coefficients (dilation 550′; orientation $\gamma = 72°$)
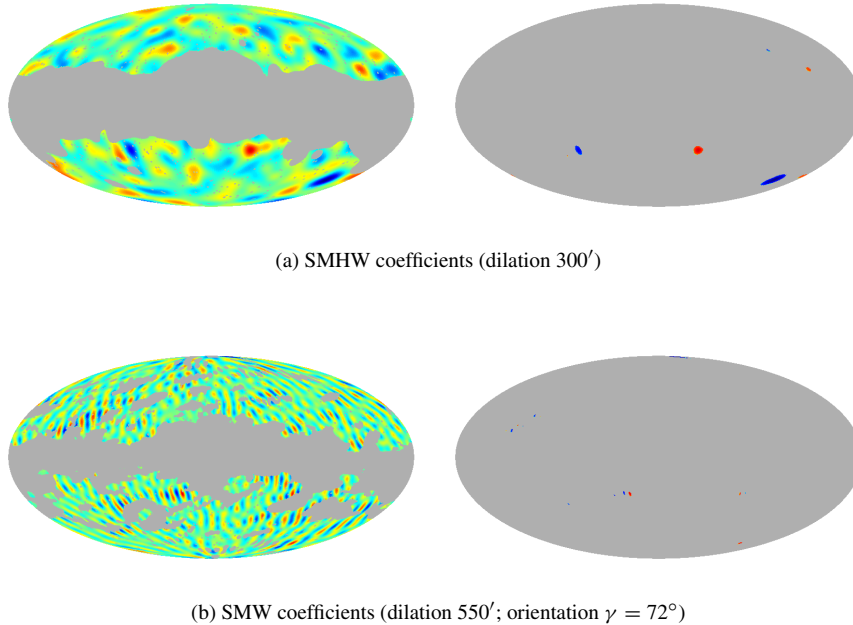
FIGURE 3   Spherical wavelet coefficient maps (left) and thresholded maps (right). To localise most likely deviations from Gaussianity on the sky, the coefficient maps exhibiting strong non-Gaussianity are thresholded so that only those coefficients above 3σ (in absolute value) remain.

Using a spherical wavelet analysis, the hypothesis that WMAP observations of the CMB are a realisation of a Gaussian random field on the sphere has been rejected. The effectiveness of the wavelet analysis on the sphere is demonstrated by the highly significant detections of deviations from Gaussianity that have been made. The source of the detected non-Gaussian signals remains unknown. Various tests to examine foreground contamination and instrumental systematics indicate that these factors are not responsible for the non-Gaussianity observed. Although it may still be the case that the deviations from Gaussianity observed are due to these factors or other astrophysical processes, if they are indeed of cosmological origin this would have profound implications for the standard cosmological model.

3.   Isotropy of the CMB

The statistical isotropy of the Universe is a fundamental assumption made in cosmology, emerging from the cosmological principle. The importance of verifying this principle cannot be overstated since many practical cosmological calculations rely heavily upon it. Strong evidence in support of the cosmological principle is provided by the highly uniform temperature of the CMB over the sky. However, small deviations of the Universe from isotropy may be imprinted in the temperature anisotropies of the CMB. If the CMB temperature anisotropies are not statistically isotropic over the sky (i.e., statistically stationary), then this may reflect the existence of an anisotropic Universe.

Recently the isotropy of the Universe has been questioned, with a number of works highlighting deviations from statistical isotropy in the WMAP data (pioneered by [20, 21, 26, 14, 19, 27, 6, 42]). Possible explanations for an anisotropic Universe arise in more exotic cosmological models, such as the so-called Bianchi models where the Universe exhibits a global shear and rotation (see e.g., [5, 23, 25, 24, 31, 8, 9]). Although some anisotropic models considered can account for some of the anomalies observed in the WMAP data, to date they fail to provide a consistent picture with concordance cosmology [25, 8].

There is no unique way of probing the isotropy of the Universe and a number of groups have applied a variety of analysis techniques. We focus here on the alignment of local CMB structures as highlighted by the steerable wavelet analysis performed by [51]. This analysis presents to the cosmological community the first application of steerable wavelets on the sphere (see [48, 50] for a discussion of steerable wavelets on the sphere). We review here the steerable wavelet analysis procedure used to probe the WMAP data for deviations from statistical isotropy and discuss the deviations that are detected.

3.1   Analysis Procedure

Under the assumption of statistical isotropy there should be no preferred directions for the orientation of local features in the CMB. A novel way of quantifying the possible alignment of CMB features has been proposed by [51]. In this analysis the number of times each direction is *seen by local CMB features* is counted. The number of times a given direction in the Universe is seen by local features provides a unique way to determine whether there exists any preferred direction on the sky towards which CMB structures are unexpectedly aligned.

Wavelets on the sphere are well suited for this type of analysis, particularly steerable wavelets. Firstly, wavelets naturally allow one to probe different scales, hence identifying different physical processes that may be responsible for violations of statistical isotropy. Secondly, steerable wavelets allow the wavelet coefficients for any continuous orientation to be computed from a set of basis orientations (see [50]). Using steerable wavelets it is therefore possible to select the orientation of the most dominant local feature.

An illustration of the technique is given in Figure 4. For each pixel the orientation of the local feature may be determined using steerable wavelets as described previously. By tracing a great circle parallel to the local orientation, the pixels that lie on this great circle may be selected as those regions *seen* by the local feature under examination. Each pixel on the great circle receives a vote proportional to the intensity the wavelet coefficient associated with the local feature. After considering the local features at each position and tallying the 'seen' pixel votes, one recovers an even signal on the sphere that may be used to test the statistical isotropy of the CMB. The signal is even (in the Cartesian coordinate system centred on the sphere) by construction since it is obtained by analysing the direction

of the local features only, without any notion about their sense (i.e., the direction vectors are headless). Under the assumption of statistical isotropy, all pixels in the resultant signal should be more-or-less 'seen' to the same degree. Simulations may be used to quantify any departures from isotropy.
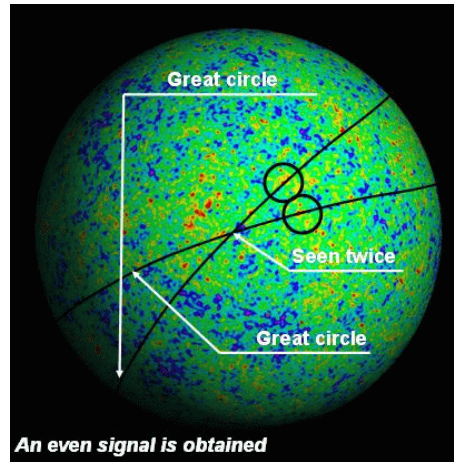

FIGURE 4   Illustration of the steerable wavelet anisotropy analysis technique. Pixels on the sky receive a weighted vote each time they are seen by CMB features (i.e., each time they lie on the great circle aligned with the local feature under examination). The votes are tallied to construct a signal on the sphere that may be used to test the statistical isotropy of the temperature fluctuations of the CMB. (This figure is a modified version of that available from Max Tegmark's web site: `http://space.mit.edu/home/tegmark/index.html`.)

3.2   Results and Discussion

The analysis procedure described above has been applied to the WMAP data, indicating a highly significant violation of statistical isotropy in the temperature fluctuations of the CMB [51, 46]. After tallying the number of times each pixel is seen and comparing this to simulations, it is possible to compute the probability that a pixel receives an anomalous number of counts, as illustrated in Figure 5(a). These results were obtained by applying the steerable wavelet basis generated from second derivatives of a Gaussian (see [50]) at a scale corresponding to an angular size on the sky of $8.3°$.

Several great circles can be identified from the most anomalous directions illustrated in Figure 5(a). In particular, one of these great circles is highlighted by the 20 most anomalous directions (identified from those pixels for which the probability of being anomalous is $> 99.99\%$) [see Figure 5(b)]. The anomalous directions are divided in two clusters, one of which lies very close to the northern ecliptic pole. It is interesting to note that this axis lies very close to the one corresponding to previously reported Equatorial north-south asymmetries (e.g., [20, 21]). In addition, the normal direction to the great circle defined for these two clusters of anomalous directions is close to the direction of the dipole[2] and the so-

---

[2]The direction of the CMB dipole represents the motion of the observer relative to the CMB reference frame and should be removed from CMB observations before cosmological inferences are drawn from the data.

(a) Anomalous probability

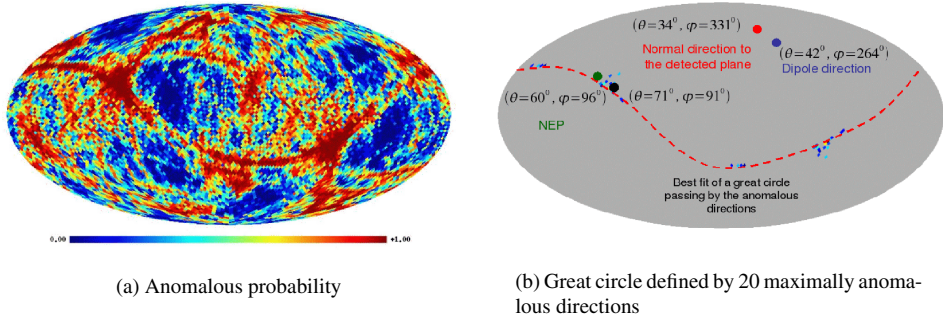(b) Great circle defined by 20 maximally anomalous directions

FIGURE 5   Anomalous directions measured in the WMAP data using the steerable wavelet analysis. In panel (a) we show the probability that a given direction on the sky is anomalous in the sense that it is seen by oriented CMB features an unusually high number of times. In panel (b) we show the great circle defined by the the 20 most anomalous directions found.

called "axis-of-evil" detected from low-multipole alignments [14, 19, 42, 27]. The steerable wavelet analysis has therefore synthesised the distinct anomalies reported previously by other methodologies, suggesting a possible interconnection.

First attempts to clarify whether this statistical anisotropy is intrinsic to CMB fluctuations or due to other sources such as foregrounds and systematics are underway. It has been shown by [46] that there does not appear to be any frequency dependence in the anisotropic signal detected and that the CMB features themselves that are aligned towards the most anomalous directions are homogeneously distributed on the sky. Both of these points seem to discard foregrounds as the source of the anisotropy.

This analysis therefore provides intriguing evidence that refutes the standard assumption that the temperature anisotropies of the CMB are statistically isotropic over the sky. Consequently, the Universe may deviate from isotropy on large scales. These findings highlight the need to explore more exotic cosmological models that could potentially better describe our Universe.

4.   Detection of the ISW Effect

Very little is know currently about the origin and nature of dark energy, yet it dominates our Universe. A consistent model of dark energy in the framework of particle physics is lacking. Indeed, attempts to predict the cosmological constant associated with dark energy by applying quantum field theory to the vacuum energy density arising from zero-point fluctuations predict a value that is too large by a factor of $\sim 10^{120}$. Despite the lack of current understanding of dark energy, the effects of a generic dark energy fluid may be modelled, describing observations of our Universe to very good approximation. Much of the current evidence of dark energy comes from recent measurements of the CMB [22] and observations of supernovae [39, 36]. At this point, confirmation of the existence of dark energy by independent physical methods is of particular interest. We review here analyses that use the integrated Sachs-Wolfe (ISW) effect [41] to independently detect and constrain dark energy.

CMB photons are blue and red shifted as they fall into and out of gravitational potential wells, respectively, as they travel towards us since emission shortly after the Big Bang. If

the gravitational potential evolves during the photon propagation, then the blue and red shifts do not cancel exactly and a net change in the photon energy occurs. The ISW effect is the integrated sum of these energy shifts over the photon path. This secondary induced CMB temperature anisotropy exists only in a non-flat Universe or in the presence of dark energy [35]. The recent WMAP data has imposed strong constraints on the flatness of the Universe [43], hence any ISW signal may be interpreted directly as a signature of dark energy.

It is difficult to isolate the contribution of the ISW effect from CMB temperature anisotropies, hence it is not feasible to detect the ISW effect solely from the CMB. Instead, as first proposed by [15], the ISW effect may be detected by cross-correlating the CMB anisotropies with tracers of the local matter distribution, such as the nearby galaxy density distribution. A detection of large-scale positive correlation is a direct indication of the ISW effect, and correspondingly, direct evidence for dark energy.

The ISW effect was first detected successfully by [7] and subsequently by many other researchers using a wide range of different analysis techniques and data-sets. Furthermore, in some analyses detections of the ISW effect are used to constrain the dark energy parameters of cosmological models. In these works the cross-correlation of the CMB with various tracers of the near Universe large scale structure is performed in either real or harmonic space, resulting in detections of the ISW effect at the 2.5σ level approximately. Recently, the cross-correlation has been evaluated in spherical wavelet space [45, 33, 37]. Since the ISW effect is localised to certain scales and positions on the sky, wavelets are an ideal tool for searching for cross-correlations due to the inherent scale and spatial localisation encoded in the analysis. The effectiveness of the wavelet analysis is demonstrated by the highly significant detections of the ISW effect made in wavelet space at greater than the 3σ level. It should be noted, however, that when information on all scales and orientations is incorporated to compute parameter constraints, the performance of the wavelet analysis is comparable to other linear techniques, as expected (assuming the fields considered are indeed Gaussian). In the remainder of this section we review the detections of the ISW effect made by [45, 33] and the corresponding constraints that are placed on dark energy parameters from these detections.

4.1   Spherical Wavelet Estimator

The correlation of the wavelet coefficients may be used as an estimator to detect any correlation between the CMB and the galaxy density distribution. A theoretical prediction of the wavelet correlation may be specified for a given cosmological model also. This is derived for azimuthally symmetric spherical wavelets by [45]. The nontrivial extension to directional wavelets is derived by [33].

Using this result it is possible to define a theoretical expected signal-to-noise ratio (SNR) for the wavelet correlation estimator. Similar expected SNRs may be defined for real and harmonic space cross-correlation estimators and are compared in [45]. In Figure 6 these expected SNRs are plotted for the various techniques. It is apparent that the wavelet estimator is superior on a large range of scales, highlighting the effectiveness of the spherical wavelet analysis.[3] Of course, when information on all scales is incorporated, the performance of the wavelet analysis is comparable to the other linear techniques. Nevertheless,

---

[3]A similar comparison is performed in [33] to compare the expected performance of various spherical wavelets.

the wavelet analysis allows one to unfold this information and to probe only those scales with high expected SNR.
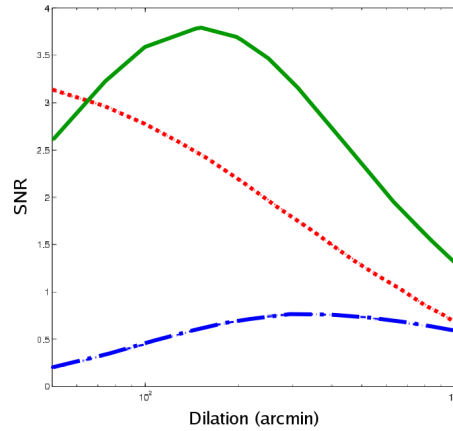

FIGURE 6   Expected SNR of cross-correlation estimators for the SMHW estimator (solid), real space estimator (dotted) and harmonic space estimator (dot-dashed). Notice the superiority of the wavelet estimator on a large range of scales.

4.2   Analysis Procedure

The analysis procedure consists of computing the wavelet correlation estimator from the wavelet coefficients of the WMAP and NRAO VLA Sky Survey (NVSS) data [13] computed for a range of scales and orientations. Only those scales where the ISW signal is expected to be significant are considered, that is scales ranging over wavelet dilation $100'$–$500'$. Anisotropic dilations are used in the analysis performed by [33] in order to further probe oriented structure in the data (see [32] for a description of anisotropic dilations on the sphere). Five evenly spaced γ orientations in the domain $[0, \pi)$ are considered.[4] Any deviation from zero in the wavelet correlation estimator for any particular scale or orientation is an indication of a correlation between the data and hence a possible detection of the ISW effect. Monte Carlo simulations are performed to construct significance measures on any detections made. Gaussian simulations of CMB data are constructed that model carefully the WMAP observing strategy also. An identical analysis is performed using the simulated CMB maps in place of the WMAP data in order to constrain the significance of any candidate detections. Finally, any detections of the ISW effect are used to constrain dark energy parameters by comparing observations to theoretical predictions made by various cosmological models.

---

[4]Identical orientations are considered at each point, in contrast to the continuous orientational analysis that could be performed using steerable wavelets. The latter approach is the focus of current work.

4.3   Results and Discussion

We review here the results obtained using the SMHW only (the numerical results obtained using other wavelets differ slightly, however the conclusions drawn from the analysis remain the same). A positive wavelet correlation outside of the 99% significance level is detected on a number of scales and orientations using the SMHW. On examining the distribution of the wavelet correlation statistics from the simulations, the correlation statistics were found to be approximately Gaussian distributed. This implies that the approximate significance of any detection of a nonzero correlation can be inferred directly from the number of standard deviations that the detections deviate by, i.e., from the N_σ level. In Figure 7 the N_σ surface is displayed in the anisotropic wavelet dilation parameter space. The maximum detection occurs at $N_\sigma = 3.9$ on wavelet scales corresponding to approximately $10°$.
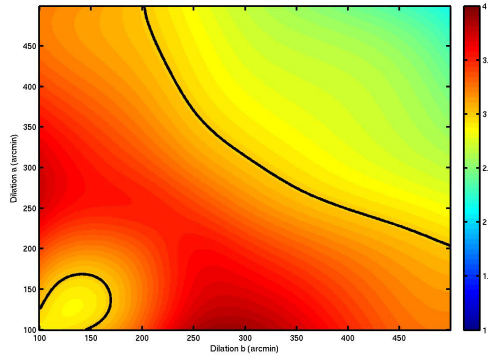

FIGURE 7   SMHW correlation N_σ surface. Contours are shown for $N_\sigma = 3$.

Foregrounds and systematics were analysed in detail and were determined *not* to be the source of the correlation detected. Furthermore, the wavelet analysis inherently allows one to localise those regions on the sky that contribute most strongly to the cross-correlation observed. After localising these regions they were determined not to be the *sole* source of correlation between the WMAP and NVSS data. This is consistent with predictions of the ISW effect; namely, that one would expect to observe weak correlations over the entire sky rather than a few strongly correlated regions. All tests indicate that the correlation detected in these works is indeed due to the ISW effect, thus providing direct and independent evidence for dark energy.

The positive detection of the ISW effect may be used to place constraints on the properties of dark energy. By comparing theoretical predictions for various cosmological scenarios with measurements made from the data it is possible to recover the probability distribution of the data given various parameters, i.e., the likelihood function. The dark energy density parameter Ω_Λ and the equation-of-state parameter w, which describes the ratio of pressure to density of the dark energy fluid, are probed in the ranges $0 < \Omega_\Lambda < 0.95$ and $-2 < w < 0$. The full likelihood and marginalised distributions are illustrated in Figure 8. The resulting parameter estimates (see Figure 8) are consistent with those made from numerous other analysis techniques and data-sets (e.g., [43]).

The effectiveness of a spherical wavelet analysis to detect the ISW effect and thus make an independent detection of dark energy has been demonstrated. Although wavelets perform
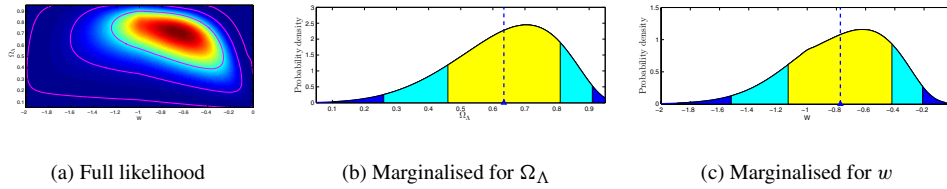
(a) Full likelihood   (b) Marginalised for Ω_Λ (c) Marginalised for w

FIGURE 8   Likelihood surfaces for parameters (Ω_Λ, w). The full likelihood surface is shown with 68%, 95% and 99% confidence contours shown also. Marginalised distributions for each parameter are shown in the remaining panels, with 68% (light-grey), 95% (grey) and 99% (dark-grey) confidence regions shown also. The parameter estimates made from the mean of the marginalised distributions are shown by the triangle and dashed line.

very well when attempting to detect the ISW effect since one may probe different scales, positions and orientations, once all information is incorporated to compute likelihoods the performance of a wavelet analysis is comparable to other linear techniques, as expected. Consequently, only weak constraints may be placed on standard dark energy parameters through the ISW effect, using wavelets or any other linear technique. Nevertheless, it is important to perform independent tests to confirm the existence of the dark energy. Moreover, an interesting avenue of future research is to investigate the use of the ISW effect and a spherical wavelet analysis to place tight constraints on nonstandard dark energy parameters, such as the dark energy sound speed [37, 47], where other techniques have failed previously.

5. Concluding Remarks

In this article we have reviewed cosmological applications of a wavelet analysis on the sphere, concentrating on analyses of the CMB. The CMB provides a unique imprint of the early Universe and as such contains a wealth of cosmological information; spherical wavelets may be used to extract this information. In the analyses reviewed herein we focus on cosmological applications that adopt the wavelet transform on the sphere first proposed by [3] and revisited by [1, 50]. We have reviewed work that has tested the assumption that the CMB temperature anisotropies are a realisation of a statistically isotropic Gaussian random field on the sphere. Highly significant deviations from both statistical isotropy and Gaussianity have been detected, suggesting possible extensions to the standard cosmological concordance model may be required. No extensions can currently account for the observed anomalies, however alternative candidates should be investigated, such as nonstandard inflationary scenarios, subdominant cosmic defect components or more exotic models, such as Bianchi contributions modelling a global rotation of the Universe. Finally, we have reviewed work that independently confirms the existence of dark energy through a detection of the ISW effect. A detection of dark energy is made at a highly significant level and is used to constrain the dark energy parameters of the cosmological concordance model. In addition to the spherical wavelet applications reviewed in detail here, wavelets on the sphere have also been used to test the global topology of the Universe [40]. This application presents an interesting avenue for further research.

The effectiveness of correctly accounting for the geometry of the sphere in the wavelet analysis of full-sky CMB data has been demonstrated by the highly significant detections of physical processes and effects that have been made in the reviewed works. These analyses have focused on the currently available WMAP data, however the forthcoming Planck data

will provide full-sky CMB maps of unprecedented precision and resolution. Future wavelet analyses of Planck data may therefore outperform the already successful analyses performed to date. Furthermore, new and novel spherical wavelet analyses of the CMB may provide further insight in understanding the nature of our Universe.

References

[1]   Antoine, J. -P. and Vandergheynst, P. (2006). Wavelets on the two-sphere and related manifolds, *J. Fourier Anal. Appl.* **13**(4), 369–386.

[2]   Antoine, J.-P., Murenzi, R., Vandergheynst, P., and Ali, S. T. (2004). *Two-Dimensional Wavelets and their Relatives,* Cambridge University Press, Cambridge.

[3]   Antoine, J.-P. and Vandergheynst, P. (1999). Wavelets on the 2-sphere: A group theoretical approach, *Appl. Comput. Harm. Anal.* **7**, 1–30.

[4]   Barreiro, R. B., Hobson, M. P., Lasenby, A. N., Banday, A. J., Górski, K. M., and Hinshaw, G. (2000). Testing the Gaussianity of the COBE-DMR data with spherical wavelets, *Mon. Not. Roy. Astron. Soc.* **318**, 475–481.

[5]   Barrow, J. D., Juszkiewicz, R., and Sonoda, D. H. (1985). Universal rotation — how large can it be? *Mon. Not. Roy. Astron. Soc.* **213**, 917–943.

[6]   Bielewicz, P., Eriksen, H. K., Banday, A. J., Górski, K. M., and Lilje, P. B. (2005). Multipole vector anomalies in the first-year WMAP data: A cut-sky analysis, *Astrophys. J.* **635**, 750–760.

[7]   Boughn, S. and Crittenden, R. (2004). A correlation of the cosmic microwave sky with large scale structure, *Nature* **427**, 45–47.

[8]   Bridges, M., McEwen, J. D., Lasenby, A. N., and Hobson, M. P. (2006). Markov chain Monte Carlo analysis of Bianchi VII$_h$ models, *Mon. Not. Roy. Astron. Soc.,* in press.

[9]   Cayón, L., Banday, A. J., Jaffe, T., Eriksen, H. K., Hansen, F. K., Gorski, K. M., and Jin, J. (2006). No higher criticism of the Bianchi-corrected Wilkinson microwave anisotropy probe data, *Mon. Not. Roy. Astron. Soc.* **369**, 598–602.

[10] Cayón, L., Jin, J., and Treaster, A. (2005). Higher criticism statistic: Detecting and identifying non-Gaussianity in the WMAP first year data, *Mon. Not. Roy. Astron. Soc.* **362**, 826–832.

[11] Cayón, L., Martínez-González, E., Argüeso, F., Banday, A. J., and Górski, K. M. (2003). COBE-DMR constraints on the nonlinear coupling parameter: A wavelet based method, *Mon. Not. Roy. Astron. Soc.* **339**, 1189–1194.

[12] Cayón, L., Sanz, J. L., Martínez-González, E., Banday, A. J., Argüeso, F., Gallegos, J. E., Górski, K. M., and Hinshaw, G. (2001). Spherical Mexican hat wavelet: An application to detect non-Gaussianity in the COBE-DMR maps, *Mon. Not. Roy. Astron. Soc.* **326**, 1243–1248.

[13] Condon, J. J., Cotton, W. D., Greisen, E. W., Yin, Q. F., Perley, R. A., Taylor, G. B., and Broderick, J. J. (1998). The NRAO VLA sky survey, *Astrophys. J.* **115**, pp. 1693.

[14] Copi, C. J., Huterer, D., and Starkman, G. D. (2004). Multipole vectors: A new representation of the CMB sky and evidence for statistical anisotropy or non-Gaussianity at $2 \leq \ell \leq 8$, *Phys. Rev. D.* **70**(4), 043515–+.

[15] Crittenden, R. G. and Turok, N. (1996). Looking for Λ with the Rees-Sciama effect, *Phys. Rev. Lett.* **76**, 575–578.

[16] Cruz, M., Cayon, L., Martínez-González, E., Vielva, P., and Jin, J. (2006). The non-Gaussian cold spot in the 3-year WMAP data, *Astrophys. J.* **655**, 11–20.

[17] Cruz, M., Martínez-González, E., Vielva, P., and Cayon, L. (2005). Detection of a non-Gaussian spot in WMAP, *Mon. Not. Roy. Astron. Soc.* **356**, 29–40.

[18] Cruz, M., Tucci, M., Martínez-González, E., and Vielva, P. (2006). The non-Gaussian cold spot in WMAP: Significance, morphology and foreground contribution, *Mon. Not. Roy. Astron. Soc.* **369**, 57–67.

[19] de Oliveira-Costa, A., Tegmark, M., Zaldarriaga, M., and Hamilton, A. (2004). Significance of the largest scale CMB fluctuations in WMAP, *Phys. Rev. D.* **69**(6), 063516–+.

[20] Eriksen, H. K., Banday, A. J., Górski, K. M., and Lilje, P. B. (2005). The N-point correlation functions of the first-year WMAP sky maps, *Astrophys. J.* **622**, 58–71.

[21] Hansen, F. K., Banday, A. J., and Górski, K. M. (2004). Testing the cosmological principle of isotropy:

Local power-spectrum estimates of the WMAP data, *Mon. Not. Roy. Astron. Soc.* **354**, 641–665.

[22] Hinshaw, G., Nolta, M. R., Bennett, C. L., Bean, R., Doré, O., Greason, M. R., Halpern, M., Hill, R. S., Jarosik, N., Kogut, A., Komatsu, E., Limon, M., Odegard, N., Meyer, S. S., Page, L., Peiris, H. V., Spergel, D. N., Tucker, G. S., Verde, L., Weiland, J. L., Wollack, E., and Wright, E. L. (2006). Three-year Wilkinson microwave anisotropy probe (WMAP) observations: Temperature analysis, *Astrophys. J.*, in press.

[23] Jaffe, T. R., Banday, A. J., Eriksen, H. K., Górski, K. M., and Hansen, F. K. (2005). Evidence of vorticity and shear at large angular scales in the WMAP data: A violation of cosmological isotropy? *Astrophys. J. Lett.* **629**, L1–L4.

[24] Jaffe, T. R., Banday, A. J., Eriksen, H. K., Gorski, K. M., and Hansen, F. K. (2006). Bianchi type VII$_h$ models and the WMAP 3-year data. `http://arXiv.org/abs/astro-ph/0606046`.

[25] Jaffe, T. R., Hervik, S., Banday, A. J., and Górski, K. M. (2006). On the viability of Bianchi type VII$_h$ models with dark energy, *Astrophys. J.* **644**, 701–708.

[26] Land, K. and Magueijo, J. (2005). Cubic anomalies in the Wilkinson microwave anisotropy probe, *Mon. Not. Roy. Astron. Soc.* **357**, 994–1002.

[27] Land, K. and Magueijo, J. (2005). Examination of evidence for a preferred Axis in the cosmic radiation anisotropy, *Phys. Rev. Lett.* **95**(7), 071301–+.

[28] Martínez-González, E. (2006). Cosmic microwave background anisotropies: The power spectrum and beyond, *ArXiv,* `http://arXiv.org/abs/astro-ph/0610162`.

[29] McEwen, J. D., Hobson, M. P., Lasenby, A. N., and Mortlock, D. J. (2005). A high-significance detection of non-Gaussianity in the WMAP 1-year data using directional spherical wavelets, *Mon. Not. Roy. Astron. Soc.* **359**, 1583–1596.

[30] McEwen, J. D., Hobson, M. P., Lasenby, A. N., and Mortlock, D. J. (2006). A high-significance detection of non-Gaussianity in the WMAP 3-year data using directional spherical wavelets, *Mon. Not. Roy. Astron. Soc.* **371**, 1583–1596.

[31] McEwen, J. D., Hobson, M. P., Lasenby, A. N., and Mortlock, D. J. (2006). Non-Gaussianity detections in the Bianchi VII$_h$ corrected WMAP 1-year data made with directional spherical wavelets, *Mon. Not. Roy. Astron. Soc.* **369**, 520–529.

[32] McEwen, J. D., Hobson, M. P., Mortlock, D. J., and Lasenby, A. N. (2007). Fast directional continuous spherical wavelet transform algorithms, *IEEE Trans. Sig. Proc.* **55**(2), 520–529.

[33] McEwen, J. D., Vielva, P., Hobson, M. P., Martínez-González, E., and Lasenby, A. N. (2007). Detection of the ISW effect and corresponding dark energy constraints made with directional spherical wavelets, *Mon. Not. Roy. Astron. Soc.* **373**, 1211–1226.

[34] Mukherjee, P. and Wang, Y. (2004). Wavelets and WMAP non-Gaussianity, *Astrophys. J.* **613**, 51–60.

[35] Peebles, P. J. E. and Ratra, B. (2003). The cosmological constant and dark energy, *Rev. Mod. Phys.* **75**, 559–606.

[36] Perlmutter, S., Aldering, G., Goldhaber, G., Knop, R. A., Nugent, P., Castro, P. G., Deustua, S., Fabbro, S., Goobar, A., Groom, D. E., Hook, I. M., Kim, A. G., Kim, M. Y., Lee, J. C., Nunes, N. J., Pain, R., Pennypacker, C. R., Quimby, R., Lidman, C., Ellis, R. S., Irwin, M., McMahon, R. G., Ruiz-Lapuente, P., Walton, N., Schaefer, B., Boyle, B. J., Filippenko, A. V., Matheson, T., Fruchter, A. S., Panagia, N., Newberg, H. J. M., and Couch, W. J. (1999). Measurements of omega and lambda from 42 high-redshift supernovae, *Astrophys. J.* **517**, 565–586.

[37] Pietrobon, D., Balbi, A., and Marinucci, D. (2006). Integrated Sachs-Wolfe effect from the cross correlation of WMAP 3year and the NRAO VLA sky survey data: New results and constraints on dark energy, *Phys. Rev. D.* **74**(4), 043524–+.

[38] Planck collaboration (2005). ESA Planck blue book, Technical Report ESA-SCI(2005)1, ESA. `http://arXiv.org/abs/astro-ph/0604069`

[39] Riess, A. G., Filippenko, A. V., Challis, P., Clocchiatti, A., Diercks, A., Garnavich, P. M., Gilliland, R. L., Hogan, C. J., Jha, S., Kirshner, R. P., Leibundgut, B., Phillips, M. M., Reiss, D., Schmidt, B. P., Schommer, R. A., Smith, R. C., Spyromilio, J., Stubbs, C., Suntzeff, N. B., and Tonry, J. (1998). Observational evidence from supernovae for an accelerating universe and a cosmological constant, *Astron. J.* **116**, 1000–1038.

[40] Rocha, G., Cayón, L., Bowen, R., Canavezes, A., Silk, J., Banday, A. J., and Górski, K. M. (2004). Topology of the Universe from COBE-DMR — a wavelet approach, *Mon. Not. Roy. Astron. Soc.* **351**, 769–778.

[41]   Sachs, R. K. and Wolfe, A. M. (1967). Perturbations of a cosmological model and angular variations of the microwave background, *Astrophys. J.* **147**, 73–90.

[42]   Schwarz, D. J., Starkman, G. D., Huterer, D., and Copi, C. J. (2004). Is the Low-ℓ microwave background cosmic? *Phys. Rev. Lett.* **93**(22), 221301–+.

[43]   Spergel, D. N., Bean, R., Doré, O., Nolta, M. R., Bennett, C. L., Hinshaw, G., Jarosik, N., Komatsu, E., Page, L., Peiris, H. V., Verde, L., Barnes, C., Halpern, M., Hill, R. S., Kogut, A., Limon, M., Meyer, S. S., Odegard, N., Tucker, G. S., Weiland, J. L., Wollack, E., and Wright, E. L. (2006). Wilkinson microwave anisotropy probe (WMAP) three-year results: Implications for cosmology, *Astrophys. J.*, in press.

[44]   Vielva, P., Martínez-González, E., Barreiro, R. B., and Sanz, J. L. (2004). Detection of non-Gaussianity in the WMAP 1-year data using spherical wavelets, *Astrophys. J.* **609**, 22–34.

[45]   Vielva, P., Martínez-González, E., and Tucci, M. (2006). Cross-correlation of the cosmic microwave background and radio galaxies in real, harmonic and wavelet space: detection of the integrated Sachs-Wolfe effects and dark energy constraints, *Mon. Not. Roy. Astron. Soc.* **365**, 891–901.

[46]   Vielva, P., Wiaux, Y., Martínez-González, E., and Vandergheynst, P. (2006). Steerable wavelet analysis of CMB structures alignment, *New Astronomy Review* **50**, 880–888.

[47]   Weller, J. and Lewis, A. M. (2003). Large scale cosmic microwave background anisotropies and dark energy, *Mon. Not. Roy. Astron. Soc.* **346**, 987–993.

[48]   Wiaux, Y., Jacques, L., and Vandergheynst, P. (2005). Correspondence principle between spherical and Euclidean wavelets, *Astrophys. J.* **632**, 15–28.

[49]   Wiaux, Y., Jacques, L., Vielva, P., and Vandergheynst, P. (2006). Fast directional correlation on the sphere with steerable filters, *Astrophys. J.* **652**, 820–832.

[50]   Wiaux, Y., McEwen, J. D., and Vielva, P. (2006). Complex data processing: Fast wavelet analysis on the sphere, *J. Fourier Anal. Appl.* **13**(4), 477–493.

[51]   Wiaux, Y., Vielva, P., Martínez-González , E., and Vandergheynst, P. (2006). Global universe anisotropy probed by the alignment of structures in the cosmic microwave background, *Phys. Rev. Lett.* **96**(15), 151303–+.

Astrophysics Group, Cavendish Laboratory, University of Cambridge, Cambridge CB3 0HE, United Kingdom
e-mail: mcewen@mrao.cam.ac.uk

Instituto de Física de Cantabria (CSIC-UC), E-39005 Santander, Spain
and
Astrophysics Group, Cavendish Laboratory, University of Cambridge, CB3 0HE Cambridge, United Kingdom
e-mail: vielva@ifca.unican.es

Signal Processing Institute, Ecole Polytechnique Fédérale de Lausanne(EPFL), CH-1015 Lausanne, Switzerland
e-mail: yves.wiaux@epfl.ch

Instituto de Física de Cantabria (CSIC-UC), E-39005 Santander, Spain
e-mail: barreiro@ifca.unican.es

Department of Physics, Purdue University, 525 Northwestern Avenue, West Lafayette, IN 47907-2036
e-mail: cayon@physics.purdue.edu

Astrophysics Group, Cavendish Laboratory, University of Cambridge, Cambridge CB3 0HE, United Kingdom
e-mail: mph@mrao.cam.ac.uk

Astrophysics Group, Cavendish Laboratory, University of Cambridge, Cambridge CB3 0HE, United Kingdom
e-mail: a.n.lasenby@mrao.cam.ac.uk

Instituto de Física de Cantabria (CSIC-UC), E-39005 Santander, Spain
e-mail: martinez@ifca.unican.es

Instituto de Física de Cantabria (CSIC-UC), E-39005 Santander, Spain
e-mail: sanz@ifca.unican.es